Pakistan Journal of Engineering and Technology (PakJET)
Multidisciplinary & Peer Reviewed
Volume: 5, Number: 1, Pages: 35- 41, Year: 2022

Hybrid Fuzzy-PI and ANFIS Controller Design for Rotor Current Control of DFIG Based Wind Turbine

Muhammad Adnan Khan[1], Ahsan Ali, and Inam-ul-Hassan Shaikh

Electrical Engineering Department, University of Engineering and Technology Taxila, Taxila., 47080, Pakistan.

[1]Corresponding author: Muhammad Adnan Khan (e-mail: madnan.khan@students.uettaxila.edu.pk).

Abstract— **Wind energy generation provides one of the best and economical solution to the growing power demand. Doubly Fed induction generator is one of the most important variable speed wind generators. Integrating advanced controllers improves its performance and efficiency. The purpose of this research work is to optimize the wind energy conversion and efficient wind power extraction by controlling rotor current. Four controllers that are PI, Fuzzy, Hybrid Fuzzy-PI and Neural network based Adaptive Neuro Fuzzy controller are designed and implemented on DFIG. Controllers' performance is assessed in terms of transients in rotor current i.e., percentage overshoot, settling time and steady state error under varying wind speed operation. Comparison of the results demonstrates that Adaptive Neuro Fuzzy controller outperforms as compared to that of Hybrid Fuzzy-PI, Fuzzy and conventional PI regarding transient response and maximum power extraction efficiency.**

Index Terms--**ANFIS controller, Doubly fed induction generator (DFIG), Hybrid Fuzzy-PI controller, Transients, Rotor current.**

I. INTRODUCTION

The demand of electricity is increasing day by day globally due to very fast growing population, economic and industrial growth. Environmental constraints also prohibit the use of fossil fuels and other conventional power generation methods. Wind power generation provides one of the best clean solution to this growing power demand due to its low cost per watt as compared to the fossil fuels, and other power generation schemes without producing any greenhouse gas and CO_2 [1]

Initially wind power generation industry was based on fixed speed wind turbines which comprised of an asynchronous squirrel-cage induction generator with multistage gearbox that are driven by wind turbine. It has simplicity of structure and manufacturing but disadvantages of reactive power consumption, no support to grid fault stability and higher mechanical stresses on the wind turbine [2]. Integration of variable wind power generation to grid affects power system operation and stability due to harmonics and flickers in the voltage, current and power. A variable speed wind generator, doubly fed induction generator (DFIG) works in wide variation range of wind speed. DFIG consists of a wound rotor induction generator. DFIG operation depends upon the wind speed. During lower wind speed, rotor will draw power from the grid, while in case of high wind speed, rotor delivers power to the grid station. DFIG are becoming popular because of their ease to implement advance features for grid integration. Soft starter in DFIG provides the grid fault through handling capability [3]. The dynamic features of DFIG mainly depends upon stator flux, rotor current and stator current. As these three parameters of DFIG are non-linear, hence increase the overall complexity of the system. One of the main parameter of DFIG is rotor current to be controlled because the output current of the wind turbine has greater overshoot, very large settling time and steady state error. These transients reduce the output power efficiency and affect the system stability [4].

There are many control strategies being studied in the literature to control the different parameters of DFIG. In [5], DFIG dynamics are improved by implementing multi-variable state feedback current controller with the feed-forward component. In another work, Model Predictive Control (MPC) approach is presented for tracking reference current of rotor by deriving reference voltage [6]. Results give both balanced and sinusoidal rotor currents in the balanced and unbalanced network. In [7], there is study of the features of Wind Energy Conversion System (WECS) with DFIG that are tracking and the robustness of three controllers i.e. PI, Fuzzy-PI, and sliding mode control (SMC) techniques are compared. In [8], fuzzy PI controller technique is presented that works for the control of active as well as reactive powers of WECS with DFIG. Results shows that by using the proposed fuzzy PI controller, dynamic response improved that have almost zero over-shoot, short settling times, and a zero steady-state error. In [9], DFIG current control techniques are presented for regulating power transmission between machines and grid. A comparison is made between the conventional PI, and Fuzzy Logic Controller (FLC) controllers with respect to the tracking, and rejection of speed disturbances. A lot of work has been done in the literature on neural networking based control for the DFIG based wind turbine [10-13]. Neural network based control technique for control of reactive power of DFIG for damping oscillations of wind system due to ground fault of power grid is proposed in [14]. Neural networks and the fuzzy-logic controls are implemented for controlling transfer of power between machines and grid [15]. To control the active and reactive power of a DFIG neural network-based control scheme is proposed in [16]. Results are also compared between PI controller and neural network-based techniques which shows that the dynamic parameters can be improved by neural network-based controller.

In this paper the impact of PI, Fuzzy, Hybrid Fuzzy-PI (combination of both Fuzzy and PI) and Neural network based Adaptive Neuro Fuzzy Inference System (ANFIS) controller on rotor current control in terms of percentage overshoot (%O.S), steady state error (SSE) and settling time τ_s is going to be analyzed. A PI Controller is designed initially that controls the SSE of the system, but system shows larger overshoot and settling time. If we implement only Fuzzy Logic Controller (FLC) controller, it reduces the system overshoot and settling time, but SSE increases more than that of PI controller results. So, a Hybrid Fuzzy-PI controller can make the SSE negligible, reduces overshoot and settling time very small. Implementing a neural network based ANFIS controller improves the transient response more than the results achieved by three stage Hybrid Fuzzy-PI controller and gives more accurate results.

II. Wind turbine and DFIG modelling

In a wind power generation system, kinetic energy of the wind is converted to mechanical energy on the turbine blades. This mechanical energy then drives the generator rotor that converts mechanical energy into electrical energy and finally fed to the grid. The configuration of wind power generation system consists of the turbine, gearbox, generator, power convertors and transformers [17]. Modelling of different components of DFIG based wind turbine can be demonstrated as follows:

A. *Wind Model*

In order to increase the overall efficiency and stability of the wind energy conversion system (WECS) quasi-steady mean wind speed plays key role. The data of wind for a specific location is collected for many years and analyzed. By Weibull distribution, wind power can be expressed as follows [18]:

$$p(v_{in}) = \frac{k}{c}\left(\frac{v_{in}}{c}\right)^{k-1} e^{-\left(\frac{v_{in}}{c}\right)^k} \quad 1$$

Where 'c' is the scale factor and 'k' the shape factor. 'v_{in}' is the instantaneous velocity of wind. By Weibull distribution, mean and average wind speed can be approximated as 5.5 m/s and 7 m/s respectively [19]. The wind kinetic energy and airflow power can be determined as follows [20]:

$$E_k = 0.5\,\rho v^2 \quad 2$$

$$P_v = 0.5\,\rho A v^3 \quad 3$$

Where 'ρ' and 'v' are the density and speed of air, and 'A' represent the area of airflow. Where wind speed v is the algebraic sum of four components [21]: average wind speed v_{av}, gust v_g , ramp v_r, and turbulence component v_t Hence:

$$v = v_{av} + v_r + v_g + v_t \quad 4$$

B. *Turbine Aerodynamic Model*

At lower wind speed and maximum aerodynamic efficiency, as wind speed increases rotor speed also increases. At higher wind speed rotor speed becomes constant at rated speed [22]. This behavior can be characterized by $C_{p-\lambda-\theta}$ curve. Where 'λ' represents tip speed ratio and 'θ' the pitch angle, and power coefficient C_p is the function of these two. Where λ can be expressed as follows [23]:

$$\lambda = \frac{\omega_t}{v} R \quad 5$$

Here 'ω_t' is rotational speed of the turbine, 'v' is the wind speed given by equation (4) and R is the blade length. The coefficient C_p can be given as:

$$C_p(\lambda,\theta) = 0.773\left(\frac{151}{\lambda} - 0.58\,\theta - 0.002\,\theta^{2.14} - 13.2\right)\left(e^{\frac{-18.4}{\lambda}}\right) \quad 6$$

Given the coefficient C_p, the output wind turbine power extracted from the wind:

$$P_{wt} = 0.5\rho A v^3 C_p(\lambda,\theta) \quad 7$$

The aerodynamic torque of the wind turbine:

$$\tau_{wt} = \frac{R}{2\lambda}\rho A v^2 C_p(\lambda,\theta) \quad 8$$

C. *Mechanical Shaft Model*

Wind turbine rotational speed can be determined by mechanical layout. The simplified two mass drive train model used for the determining the relationship between torque and rotational speed is shown in Fig. 1. 'τ_{shaft}' represents the torque of the turbine in fast speed shaft while 'τ_e' represents electrical torque of the generator. Similarly, 'ω_τ' represents fast speed shaft rotational speed while 'ω_{mec}' represents mechanical rotating speed of generator. If turbine toque is expressed as 'τ_T' and angular speed as 'ω_T', we have the following relationship [24]:

$$\tau_{shaft} = \frac{\tau_T}{N} \quad 9$$

$$\omega_\tau = N\,\omega_T \quad 10$$

$$J_\tau \frac{d\omega_\tau}{dt} = \tau_{shaft} - D_\tau \omega_\tau - \tau_e \quad 11$$

$$J_e \frac{d\omega_{mec}}{dt} = \tau_e - D_e \omega_{mec} + \tau_{shaft} \quad 12$$

$$\frac{d\tau_e}{dt} = k\,(\omega_\tau - \omega_{mec}) + D\left(\frac{d\omega_\tau}{dt} - \frac{d\omega_{mec}}{dt}\right) \quad 13$$

Here 'J_τ' and 'J_e' represents the inertia of turbine shaft and generator shaft of the respectively. D_τ represents the aerodynamic resistance of wind blades, D_e represents the friction and windage losses and D is the damping co-efficient that occurs due to difference between the turbine shaft and generator rotor.

D. *Gearbox Model*

For a single stage gearbox system usually a gear ratio of 6 is chosen. However, a higher gear ratio is suggested. It is economical to use higher gear ratio gear box for more stages. 1% of the rated power loss for a single stage gearbox is reasonable. The power losses in the gear box are mathematically expressed as follows [25]:

$$P_g = P_{gl}\frac{n}{n_{rated}} \qquad 14$$

Here P_{gl} represents the losses at rated speed. n represents the mechanical speed of the generator in (rev/min).

E. Generator Model

In this research a 2.0MW wound rotor induction generator is selected. If stator and rotor resistances are represented by r_s and r_r and stator and rotor flux in abc reference frame are represented by λ_{abcs} and λ_{abcr} The 3-phase stator and rotor voltage equations in a, b, c frame can be expressed as [26] :

$$v_{abcs} = r_s i_{abcs} + p\,\lambda_{abcs} \qquad 15$$

$$v_{abcr} = r_r i_{abcr} + p\,\lambda_{abcr} \qquad 16$$

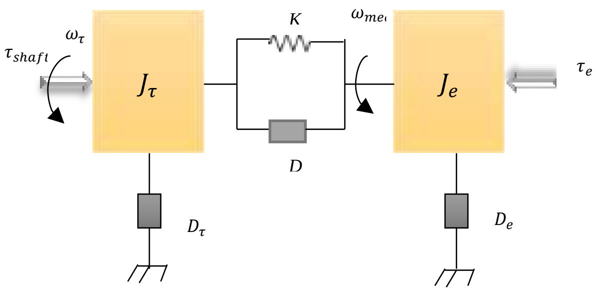

FIGURE 1: Two mass drive train model

Rotor and stator voltages into d-q reference frame [26] :

$$v_{qs} = L_s\frac{di_{qs}}{dt} + M\frac{di_{qr}}{dt} + L_s\omega_s i_{ds} + r_s i_{qs} + M\,\omega_s i_{rd} \qquad 17$$

$$v_{ds} = L_s\frac{di_{ds}}{dt} + M\frac{di_{dr}}{dt} - L_s\omega_s i_{qs} + r_s i_{ds} + M\,\omega_s i_{rq} \qquad 18$$

$$v_{qr} = M\frac{di_{qs}}{dt} + L_r\frac{di_{qr}}{dt} + s\omega_s(Mi_{ds} + L_r i_{dr}) + r_r i_{qr} \qquad 19$$

$$v_{dr} = M\frac{di_{ds}}{dt} + L_r\frac{di_{dr}}{dt} - s\omega_s(Mi_{qs} + L_s i_{qr}) - r_r i_{dr} \qquad 20$$

where ω_s in Fig. 1, represents the normal grid frequency and s is the slip. L_s and L_r represents the stator and rotor inductance and M represents the mutual inductance. The per unit electromagnetic torque can be given as follows:

$$T_e = L_m(i_{qs}\,i_{dr} - i_{ds}\,i_{dr}) \qquad 21$$

Active and reactive power losses of DFIG based wind turbine can be determined as follows:

$$P_s = \frac{3}{2}(v_{ds}\,i_{ds} + v_{qs}\,i_{qs}) \qquad 22$$

$$Q_s = \frac{3}{2}(v_{qs}\,i_{ds} - v_{ds}\,i_{qs}) \qquad 23$$

$$P_r = \frac{3}{2}(v_{dr}\,i_{dr} + v_{qr}\,i_{qr}) \qquad 24$$

$$Q_r = \frac{3}{2}(v_{qr}\,i_{dr} - v_{dr}\,i_{qr}) \qquad 25$$

III. Control System Design and Implementation

One of the prime objective of the designed controller is to improve the efficiency of the wind power generating system. Block diagram representation of the proposed system is drawn in Fig. 2. Here controller represents the proposed controllers to be implemented. First of all, PI and Fuzzy logic controller are to be designed to meet the performance requirements. Then a hybrid of Fuzzy and PI is implemented. Finally, an ANFIS controller is to be designed and compared results with Hybrid Fuzzy-PI. Controllers are to be designed on MATLAB/SIMULINK at sampling frequency of 10 KHz. There is always an lower and upper limit for which wind turbine can work known as sub-synchronous and super synchronous mode. For wind speed more than the super synchronous mode pitch control is to be encompassed. Different parameters and specifications used in simulation for DFIG based wind turbine are given in Table 1. Aerodynamic torque can be expressed from (8) by substituting $A = \pi R^2$and v from (5) [27]:

$$\tau_{wt} = \frac{1}{2}\rho\pi{\omega_m}^2\left(\frac{R^5}{\lambda^3{}_{opt}}\right)C_{p,max} \qquad 26$$

Where the optimal values selected in this design for λ_{opt} and $C_{p,max}$ are 0.44 and 7.2 respectively. The electromagnetic torque can be given as:

$$\tau_e = {}^{-\tau_{\omega T}}\!/_{N^3} \qquad 27$$

Here N represents the gearbox ratio. From the equation it is clear that the electromagnetic torque is directly proportional to the τ_{wt} and inversely proportion to that of gearbox ratio.

Rotor voltages can be expressed in the d-q reference frame as given in eq (28) – (29) while considering stator flux zero as follows [28]:

$$v_{dr} = R_r i_{dr} + \sigma L_r\frac{di_{dr}}{dt} - \omega_r\sigma L_r i_{qr} + \frac{L_m}{L_s}\frac{d|\varphi|}{dt} \qquad 28$$

$$v_{qr} = R_r i_{qr} + \sigma L_r\frac{di_{qr}}{dt} + \omega_r\sigma L_r i_{dr} + \omega_r\frac{L_m}{L_s}|\varphi| \qquad 29$$

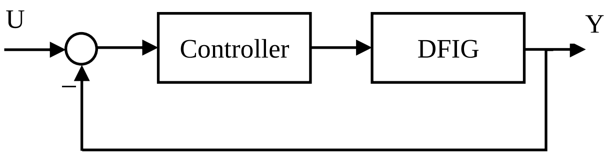

FIGURE 2: Block diagram representation.

Wind turbine system cannot be integrated with the grid until it does not meet the grid requirements. Else system will become unstable that will cause imbalance of active and reactive power due to which larger voltage drop will occur. Instability might cause a complete blackout of power system. Wind turbines usually supply variable power to grid system depending upon the wind speed. During normal wind speed, wind farm becomes a generator supplying active power to the grid system. While in case of very low wind speed or very high wind speed wind turbines are disconnected from the grid and kept in idle mode until wind speed becomes normal.

Table I: Simulated Model Parameters

Parameter Name	Value
Rated speed (n)	1500 rpm
Stator voltage (V_s)	690V
Rated rotor voltage	2070 V
Stator rated current (I_s)	1.8 A
Generator Rated Power	2.0 MW
Rated electromagnetic Torque (τ_e)	12732 N.m
Turn ratio (U)	1/3
Stator frequency (f)	50 Hz
Rotor Resistance	2.9 mΩ
Maximum Slip (S_{max})	1/3
Stator and Rotor Inductance	2.6 mH
Magnetizing Inductance (L_m)	2.5 mH
Leakage Inductance (L_l)	0.087 mH
Stator resistance	2.6 mΩ
No. of Poles	2
DC Bus voltage	325 V

A. PI Controller Design and Implementation

Two PI controller are to be designed to control two current components d and q axis rotor currents by trial-and-error method and optimized by Ziegler-Nichols tuning method to get maximum power output. The optimum controller gain that gives maximum power extraction are k_p =0.5 and k_i =500. Simulation results for PI controller with average wind speed of 8m/s controller are shown in Fig. 3. At a specific rotor speed (say 143 rad/sec) torque is 5390 N.m and rotor current is 1285A from steady state simulations. After implementing PI controller torque is near around the steady state value at speed of 143 rad/sec. Hence system is verified. Here we set $i_d = 0$ to get perfect control of i_q which represents the rotor current. It can be observed from Table 2 that the PI controller has minimizes the SSE to 0.014 seconds and 0.016 seconds for i_q and i_d respectively but overshoot and settling time are quite high. So, there is need to implement an efficient controller that can enhance the transients in rotor current to get maximum power output. As settling time of rotor current components is more than 5 seconds, simulations are performed for 10 seconds.

B. Fuzzy Logic Controller Design and Implementation

In large scale systems Fuzzy logic controller is considered to be one of the effective controllers. In electronic system it has large number of application to enhance the transients in system output response [5]. In this design two separate Fuzzy controllers are used for the fuzzification of rotor current components i_{qr} and i_{dr}.

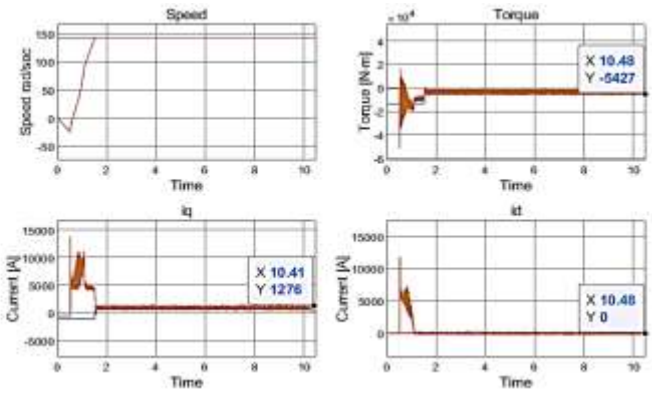

FIGURE 3: Simulation results with implementation of PI controller

Simulation results after implementing the Fuzzy controller are shown in Fig. 4. From the simulation results it can be observed that overshoot has been reduced to a great extent that is 322 for i_d and 536 for i_q. Also settling time has been reduced to 6.8 seconds and 1.97 seconds for i_d and i_q respectively. However, it increases the SSE more than that of PI controller. SSE with Fuzzy controller is 0.81 and 0.58 for i_d and i_q respectively.

C. Hybrid Fuzzy-PI Controller Design and Implementation

The simulation results of Fuzzy controller in Table. 2 shows that the overshoot and settling time has been reduced while it has increased the SSE compared with PI controller. So, a hybrid of the two Fuzzy and PI is implemented, so that PI controller reduces the SSE and Fuzzy controller will improves the settling time and overshoot. The Simulation results after implementing the designed hybrid controller are shown in Fig. 5.

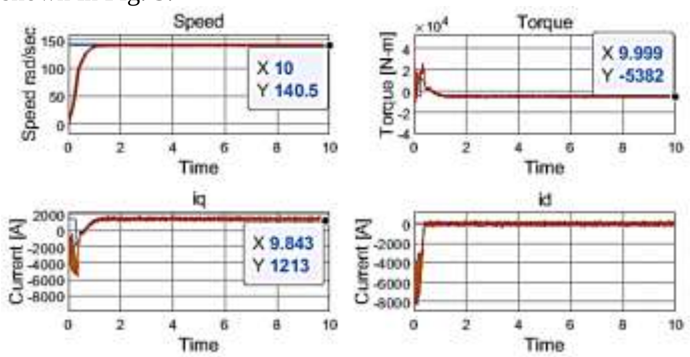

FIGURE 4. Simulation results with implementation of Fuzzy controller

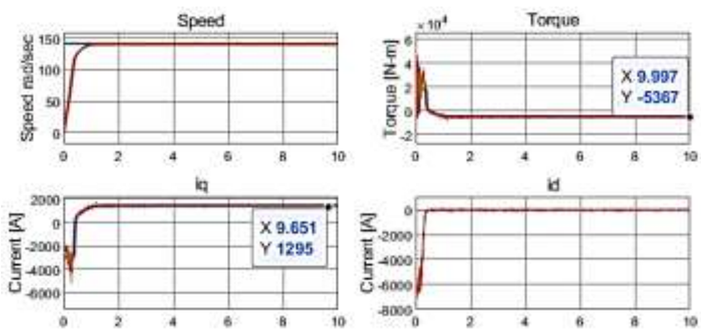

FIGURE 5. Simulation results with implementation of Fuzzy-PI controller

Simulation results with designed hybrid controller in Table. 2 show that SSE of the rotor current components i_{qr} and i_{dr}

have been reduced to 0.004 and 0.0031 respectively. Also, overshoot has been reduced to 310 and 806 while settling time in the response are reduced to 5.9 seconds and 1.67 seconds for i_{dr} and i_{qr} respectively.

D. ANFIS Controller Design and Implementation

Adaptive neural networking is gaining popularity now a days in nonlinear control system. Neuro-Fuzzy combines the advantages of both fuzzy logic and neural network. Basic structure of ANFIS system is a rule model by which input is mapped into a membership function. maps the input characteristics to an input membership function which are converted to rules. These rules are mapped to the output characteristics, which are then mapped to the output membership function. Finally, output membership function is converted to a single decision value. It computes the member function that best allow the associated fuzzy inference system to track the given input/output data. ANFIS uses a back propagation and least square estimation for the estimation of input/output membership functions [29]. In our design input to the controller are error signal and rate of change of error. Structure of the designed ANFIS controller and simulation results are shown in Fig. 6 and Fig. 7 respectively. From simulation graphs of the rotor current component, it can be inferred that ANFIS controller has much better performance than Fuzzy and Hybrid Fuzzy-PI controller because it has reduced the SSE along with the settling time τ_s and overshoot has been reduced.

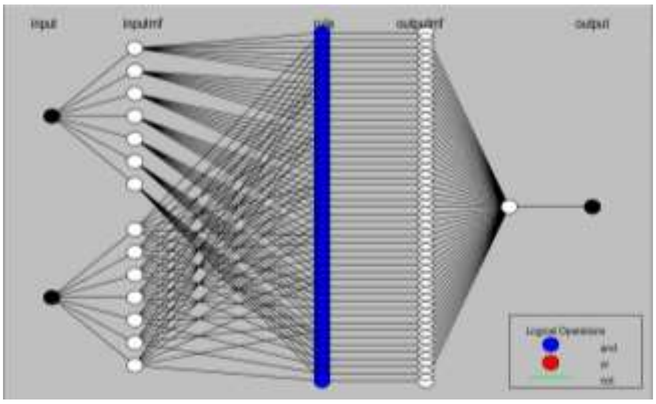

FIGURE 6: Designed ANFIS controller

Results of ANFIS controller simulation in Table. 2 demonstrates that percentage overshoot (%O.S) has been reduced to a great extent, that is 130. Also, SSE is equal to that of Hybrid controller. Settling time τ_s has been reduced as compared to the PI, Fuzzy and Hybrid Fuzzy-PI controller. It can be inferred that ANFIS controller has better performance as compared to the PI, Fuzzy and Hybrid Fuzzy-PI.

IV. Comparison of Results

In this section, the performance of the proposed four controllers PI, Fuzzy, Hybrid Fuzzy-PI and ANFIS controller for efficient power extraction while controlling the transients in rotor current of DFIG is evaluated. Fig. 8 and Fig. 9 shows the rotor current components i_q and i_d using the four controllers. It can be easily observed that ANFIS controller has good performance in tracking the desired refence current.

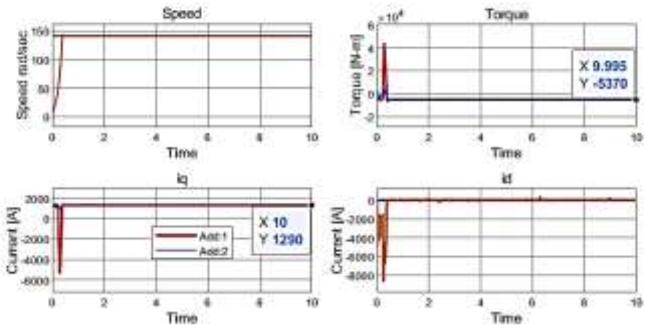

FIGURE 7. Simulation results with implementation of ANFIS controller

V. Comparison of Results

In this section, the performance of the proposed four controllers PI, Fuzzy, Hybrid Fuzzy-PI and ANFIS controller for efficient power extraction while controlling the transients in rotor current of DFIG is evaluated. Fig. 8 and Fig. 9 shows the rotor current components i_q and i_d using the four controllers. It can be easily observed that ANFIS controller has good performance in tracking the desired refence current. Hybrid Fuzzy-PI controller first required to tune PI controller and then design a Fuzzy controller. But still ANFIS controller has best performance with lower overshoot, SSE and settling time τ_s than other three controllers. Table. II represents the simulation results of the PI, Fuzzy, Hybrid Fuzzy-PI and ANFIS controller. A PI Controller is used for pitch control in DFIG and that also controls the rotor current. To the best of author's knowledge after thoroughly going through the literature, there is no such a study that evaluate the overshoot, settling time and steady state error impacts on output power efficiency. Investigating the transient characteristics of the conventional PI controller, it can be observed from Table. 2 PI has very small SSE but very large value of %O.S and settling time. So, there is need to implement a control strategy that improves the overshoot and settling time. Fuzzy controller has lower overshoot value, but it has larger value of SSE than PI controller. Hybrid controller still have a larger value of overshoot. ANFIS controller has very small settling time and overshoot as compared to the other three controllers. Extracted power from wind turbine generation system at different wind speed (7m/s to 11m/s) after the implementation of four controllers is shown in Fig. 10. PI controller shows degradation and power extracted is 1400 KW at 11 m/s. Implementing Fuzzy controller gives output power of 1682 KW while in case of Hybrid Fuzzy-PI it is 1725 KW. Extracted power achieved rated power using ANFIS controller which is 2MW at nominal wind speed of 11 m/s. Hence extracted power from ANFIS is maximum and as it is clear from Fig. 11 that the output power from ANFIS controller is efficient as compared to any other controller. Power extracted from the simulated DFIG with different designed controller is shown in Fig. 11. PI and Hybrid controller has larger %O.S as compared to ANFIS and Fuzzy controllers. While Fuzzy controller on the other hand has larger settling time τ_s as compared to Hybrid controller. Hybrid Fuzzy-PI controller controls the settling time and SSE, But overshoot is larger as compared to fuzzy in case of i_{qr} as given in Table 2. ANFIS controller outperforms regarding transient control and power extraction efficiency.

TABLE II: Comparison of results for different Controllers

Parameters	i_{qr}				i_{dr}			
	PI	**Fuzzy**	**Hybrid Fuzzy-PI**	**ANFIS**	**PI**	**Fuzzy**	**Hybrid Fuzzy-PI**	**ANFIS**
%O.S	14101	536	806	106	16001	322	310	120
Settling Time τ_s(s)	4.1	1.97	1.67	0.78	7.5	6.8	5.9	5.9
SSE	0.014	0.58	0.004	0.002	0.016	0.81	0.0031	0.0031

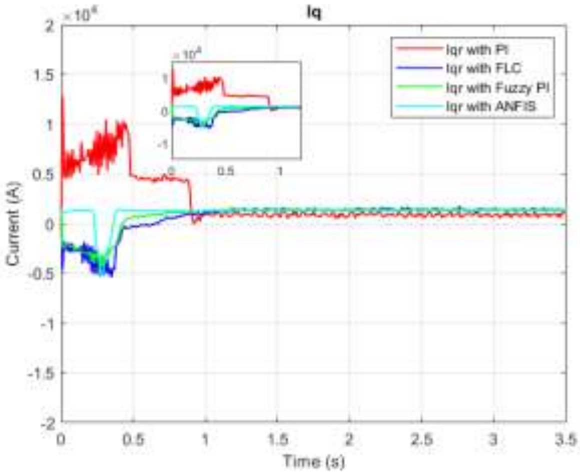

FIGURE 8: Comparison of rotor current component i_{qr} for different Controllers

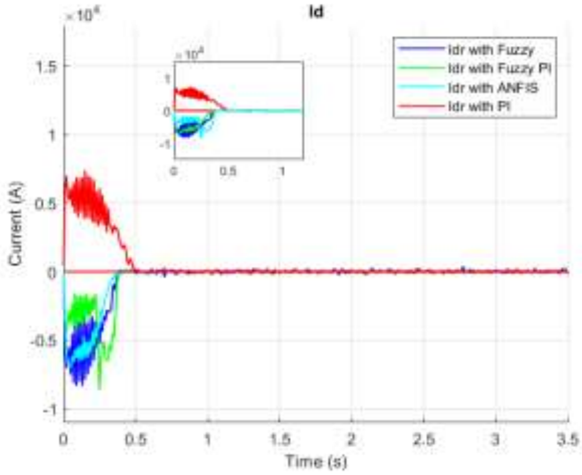

FIGURE 9. Comparison of rotor current component i_{dr} for different controllers

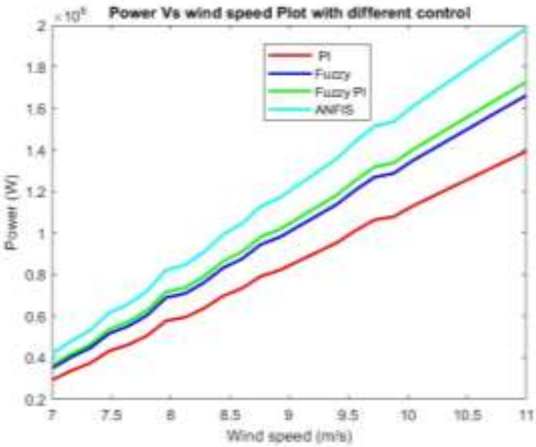

FIGURE 10. Power extracted Vs wind speed after Implementing different controllers.

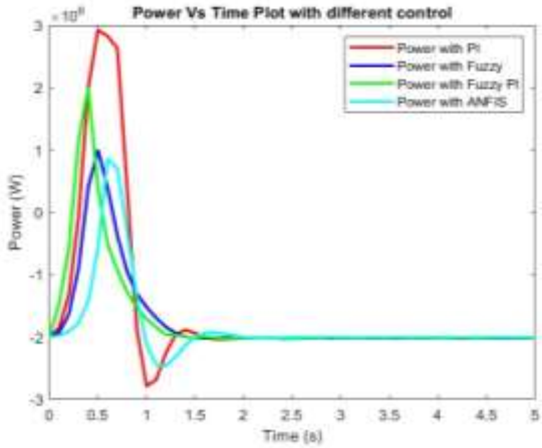

FIGURE 11: Power extracted with implementing the proposed

VI. CONCLUSION

A variable speed DFIG based wind turbine under variable wind speed operation is studied in this research. Implementation of PI, Fuzzy, Hybrid Fuzzy-PI and ANFIS controller for the rotor current control on a 2 MW wind turbine system is presented. Simulation on MATLAB/SIMULINK are carried out to investigate the performance evaluation of proposed controller in terms of transient characteristics (percentage overshoot, settling time, SSE) and efficient power extraction. PI controller has larger overshoot and very small SSE. Implementing Fuzzy controller control the overshoot of the current but increases the SSE. Hybrid of Fuzzy and PI reduces the SSE, Settling time and overshoot very small. However, the overshoot little bit more than that of Fuzzy controller results for i_q component. But SSE is negligibly small. ANFIS controller has smaller value of overshoot as compared to other three controllers and shows better results for settling time and SSE.

In future, other advanced control technique and optimal controls could be utilized for rotor current control to improve the efficiency of wind power generation system. Also, frequency control strategies can be implemented to control the rotor current of DFIG based wind turbine.

References

[1] A. L. M. Abdali, B. Yakimovich, and V. J. e. Kuvshinov, "Hybrid power generation by using solar and wind energy," energy, vol. 2, no. 3, pp. 26-31, 2018.

[2] K. A. Naik and C. P. J. E. Gupta, "Output power smoothing and voltage regulation of a fixed speed wind generator in the partial load region using STATCOM and a pitch angle controller," *Energies*, vol. 11, no. 1, p. 58, 2018.

[3] A. Dida, F. Merahi, S. J. C. Mekhilef, and E. Engineering, "New grid synchronization and power control scheme of doubly-fed induction generator based wind turbine system using fuzzy logic control," *Computers & Electrical Engineering*, vol. 84, p. 106647, 2020.

[4] B. Qin and H. J. I. A. Sun, "State dependent riccati equation based rotor-side converter control for doubly fed wind generator," *IEEE Access*, vol. 6, pp. 27853-27863, 2018.

[5] A. G. Abo-Khalil, A. Alghamdi, I. Tlili, and A. M. J. I. R. P. G. Eltamaly, "Current controller design for DFIG-based wind turbines using state feedback control," *IET Renewable Power Generation*, vol. 13, no. 11, pp. 1938-1948, 2019.

[6] Y. Zhang and J. Jiao, "Model predictive rotor current control for doubly fed induction generators under unbalanced grid voltages," in *2018 IEEE International Power Electronics and Application Conference and Exposition (PEAC)*, 2018, pp. 1-5: IEEE.

[7] L. Saihi, B. Berbaoui, and H. J. M. J. o. E. E. Glaoui, "Robust control H∞ fuzzy of a doubly fed induction generator integrated to wind power system," *Majlesi Journal of Electrical Engineering*, vol. 14, no. 1, pp. 59-69, 2020.

[8] C. Rocha-Osorio, J. Solís-Chaves, L. L. Rodrigues, J. A. Puma, and A. J. I. t. Sguarezi Filho, "Deadbeat–fuzzy controller for the power control of a Doubly Fed Induction Generator based wind power system," *ISA transactions*, vol. 88, pp. 258-267, 2019.

[9] A. Thakallapelli, S. Kamalasadan, K. M. Muttaqi, and M. T. J. I. T. o. I. A. Hagh, "A synchronization control technique for soft connection of doubly fed induction generator based wind turbines to the power grids," *IEEE Transactions on Industry Applications*, vol. 55, no. 5, pp. 5277-5288, 2019.

[10] H. Benbouhenni, Z. Boudjema, and A. J. I. J. o. S. G.-i. Belaidi, "A direct power control of the doubly fed induction generator based on the three level NSVPWM technique," *Elektrotehniski Vestnik*, vol. 3, no. 4, pp. 216-225, 2019.

[11] N. G. Lantewa and N. Magaji, "Control of doubly fed induction generator of variable speed wind turbine system using neural network," *International Conference and Utility Exhibition on Green Energy for Sustainable Development (ICUE)*, 2018, pp. 1-6: IEEE.

[12] S. Karad and R. J. A. o. C. M. i. E. Thakur, "Recent trends of control strategies for doubly fed induction generator based wind turbine systems: A comparative review," *Archives of Computational Methods in Engineering*, vol. 28, no. 1, pp. 15-29, 2021.

[13] S. R. D. Stallon and M. N. J. I. T. o. E. E. S. Rajkumar, "Improving the performance of grid-connected doubly fed induction generator by fault identification and diagnosis: A kernel PCA-ESMO technique," *International Transactions on Electrical Energy Systems*, vol. 31, no. 4, p. e12844, 2021.

[14] D. Hore and R. J. W. E. Sarma, "Neural network–based improved active and reactive power control of wind-driven double fed induction generator under varying operating conditions," *Wind Engineering*, vol. 42, no. 5, pp. 381-396, 2018.

[15] Y. Ibrahim, S. Kamel, A. Rashad, L. Nasrat, and F. J. I. J. I. M. A. I. Jurado, "Performance Enhancement of Wind Farms Using Tuned SSSC Based on Artificial Neural Network," *Int. J. Interact. Multim. Artif. Intell.*, vol. 5, no. 7, pp. 118-124, 2019.

[16] G. V. Madhav, Y. J. I. J. o. E. Obulesu, and C. Engineering, "A New Hybrid Artificial Neural Network Based Control of Doubly Fed Induction Generator," *International Journal of Electrical & Computer Engineering International Journal of Electrical & Computer Engineering*, vol. 5, no. 3, 2015.

[17] R. Akbari, A. Izadian, and R. S. J. I. T. o. I. A. Weissbach, "Quasi self-excited DFIG-based wind energy conversion system," *IEEE Transactions on Industry Applications*, vol. 57, no. 3, pp. 2816-2824, 2021.

[18] M. S. Nazir, N. Ali, T. Yongfeng, A. N. Abdalla, and H. M. J. J. J. o. E. S. Nazir, "Renewable Energy based Experimental Study of Doubly Fed Induction Generator: Fault case analysis," *Journal of Electrical Systems*, vol. 16, no. 2, 2020.

[19] H. Sun and H. J. R. E. Yang, "Numerical investigation of the average wind speed of a single wind turbine and development of a novel three-dimensional multiple wind turbine wake model," *Renewable Energy*, vol. 147, pp. 192-203, 2020.

[20] A. Bektache, B. J. I. j. o. e. p. Boukhezzar, and E. systems, "Nonlinear predictive control of a DFIG-based wind turbine for power capture optimization," *International journal of electrical power & Energy systems*, vol. 101, pp. 92-102, 2018.

[21] Z. Shu *et al.*, "Assessing wind gust characteristics at wind turbine relevant height," *Journal of Renewable and Sustainable Energy*, vol. 13, no. 6, p. 063308, 2021.

[22] A. Sedaghat, F. Alkhatib, A. Eilaghi, M. Sabati, L. Borvayeh, and A. J. E. P. Mostafaeipour, "A new strategy for wind turbine selection using optimization based on rated wind speed," *Energy Procedia*, vol. 160, pp. 582-589, 2019.

[23] Y. Xu, P. Chen, X. Zhang, and D. J. E. Yang, "An Improved Droop Control Scheme of a Doubly-Fed Induction Generator for Various Disturbances," *Energies*, vol. 14, no. 23, p. 7980, 2021.

[24] R. Rink and R. Małkowski, "Real-time hybrid model of a wind turbine with doubly fed induction generator," *IEEE 60th International Scientific Conference on Power and Electrical Engineering of Riga Technical University (RTUCON)*, 2019, pp. 1-5: IEEE.

[25] S. Abdi, S. Sharifzadeh, and S. Amiri, "Reliability Model Development for Wind Turbine Drivetrain with Brushless Doubly-Fed Induction Machine as Generator," *22nd IEEE International Conference on Industrial Technology (ICIT)*, 2021, vol. 1, pp. 228-233: IEEE.

[26] M. Hallak, M. Hasni, and M. Menaa, "Modeling and control of a doubly fed induction generator base wind turbine system," *International Conference on Electrical Sciences and Technologies in Maghreb (CISTEM)*, 2018, pp. 1-5: IEEE.

[27] O. Barambones, J. A. Cortajarena, I. Calvo, J. M. G. de Durana, P. Alkorta, and A. J. R. e. Karami-Mollaee, "Variable speed wind turbine control scheme using a robust wind torque estimation," *Renewable energy*, vol. 133, pp. 354-366, 2019.

[28] A. R. Kumhar, "Vector Control Strategy to Control Active and Reactive Power of Doubly Fed Induction Generator Based Wind Energy Conversion System," *2nd International Conference on Trends in Electronics and Informatics (ICOEI)*, 2018, pp. 1-9: IEEE.

[29] J. Su, Y. Chen, D. Zhang, and Y. J. I. T. o. P. E. Kang, "Full-Parameter Identification Model Based on Back Propagation Algorithm for Brushless Doubly Fed Induction Generator," *IEEE Transactions on Power Electronics*, vol. 35, no. 10, pp. 9953-9958, 2020.